# NMR-Detected Order in Core Residues of Denatured Bovine Pancreatic Trypsin Inhibitor†

Elisar Barbar,*,‡ Michael Hare,‡ Moses Makokha,‡ George Barany,§ and Clare Woodward||

*Department of Chemistry and Biochemistry, Ohio University, Athens, Ohio 45701, Department of Chemistry, University of Minnesota, Minneapolis, Minnesota 55455, and Department of Biochemistry, University of Minnesota, St. Paul, Minnesota 55108*

*Received March 9, 2001; Revised Manuscript Received June 12, 2001*

ABSTRACT: The NMR characteristics of $[14-38]_{Abu}$, a synthetic variant of BPTI that is partially folded in aqueous buffer near neutral pH, support a model of early folding events which begin with stabilization of the nativelike, slow exchange core [Barbar, E., Hare, M., Daragan, V., Barany, G., and Woodward, C. (1998) *Biochemistry 37*, 7822−7833 (*1*)]. In partially folded $[14-38]_{Abu}$, urea denaturation profiles for representative amide protons show that global unfolding is non-two-state and that core residues require a higher concentration of urea to unfold. Dynamic properties of pH-denatured $[14-38]_{Abu}$ and fully reduced and unfolded BPTI analogue were determined from heteronuclear NMR relaxation measurements at similar solution conditions. Differences at various sites in the polypeptide chain were evaluated from spectral density functions determined from $T_1$, $T_2$, and steady-state heteronuclear NOE data. Although denatured $[14-38]_{Abu}$ contains no persistent secondary structure, its most ordered residues are those that, in native BPTI, fold into the slow exchange core. The fully reduced analogue is significantly more mobile and shows less heterogeneous dynamics, but at 1 °C, restricted motion is observed for residues in the central segments of the polypeptide chain. These observations indicate that there is a developing core or cores even in highly unfolded species. Apparently the effect of 14−38 disulfide on unfolded BPTI is to preferentially order and stabilize residues in the core.

The structure and dynamics of intermediates formed during protein folding are refractory to characterization because they are heterogeneous and their lifetimes typically fall below the resolution of conventional techniques. The structural heterogeneity is related to the multiple, parallel pathways for folding from a denatured ensemble to a native state; intermediates formed during the process are not well described as one or a few average structures, but rather as families of conformations (*2*−*4*). To produce proteins representative of the conformational ensembles transiently formed at various stages of folding, a number of methods are used to obtain denatured forms that are unfolded to various degrees (*5*−*9*). Our approach is to use chemical synthesis to prepare protein variants that are partially folded or fully denatured near physiological pH without added denaturant, so that comparisons among them at similar temperatures and buffer conditions are simplified (*10*, *11*). For very early stages of protein folding, our models are unfolded variants of BPTI[1] that have no secondary or tertiary structure detected by CD or NMR. These include $[R]_{Abu}$ in which all six cysteines are replaced by Abu, and unfolded $[14-38]_{Abu}$ that has been denatured by pH, temperature, or amino acid replacement. For intermediates populated at middle stages of folding, our model is partially folded $[14-38]_{Abu}$, a synthetic variant of BPTI with four of the six cysteines replaced by α-amino-butyric acid (Abu) which is isosteric with cysteine.

In the course of our studies, a general hypothesis has emerged, that the slow exchange core is the folding core (*12*). Slow exchange refers to the hydrogen isotope exchange of amide NH groups with solvent water. If the hypothesis is true, the implication is that regions of the polypeptide chain that most favor ordered structure before and during folding are those that after folding compose the slow exchange core. Ensuing questions include the following. Is ordered structure detected in core residues of fully unfolded proteins? In partially folded species, how do core residues differ from other residues with regard to structure, dynamics, and behavior during global denaturation by temperature or urea?

The question of nascent ordered structure in fully unfolded BPTI is answered in part by previous studies and in part by experiments reported here. Table 1 lists the unfolded and partially folded variants of BPTI studied here and earlier.

† This work was supported by grants from the Ohio Cancer Research Associates (E.B.), the NIH [GM26242 (C.W.), NIH GM51628 (G.B. and C.W.)], and the American Cancer Society (M.H.).

* Correspondence should be addressed to this author at the Department of Chemistry and Biochemistry, Ohio University, Athens, OH 45701. Tel: (740) 593-1751, Fax: (740) 593-0148, Email: barbar@ohio.edu.

‡ Ohio University.

§ University of Minnesota, Minneapolis.

|| University of Minnesota, St. Paul.

[1] Abbreviations: BPTI, bovine pancreatic trypsin inhibitor; Abu, α-amino-*n*-butyric acid; $[14-38]_{Abu}$, BPTI with the 14−38 disulfide intact and the other four cysteines replaced with Abu; $D_{(14-38)}$, pH-denatured $[14-38]_{Abu}$; $[R]_{Abu}$, BPTI with all six cysteines replaced with Abu; PF, partially folded ensemble; $P_f$, more folded conformations of PF; $P_d$, more disordered conformations of PF; D, denatured ensemble; HSQC, heteronuclear single quantum coherence; $T_1$, longitudinal relaxation time constant; $T_2$, transverse relaxation time constant.

10.1021/bi010483z CCC: $20.00 
Published on Web 07/18/2001

Table 1: Partially Folded and Denatured BPTI Species[a]

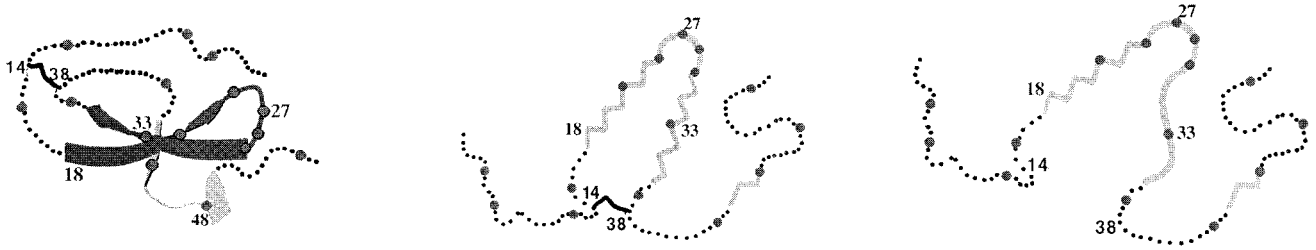


| partially folded $[14-38]_{Abu}$, PF[b] | | denatured $[14-38]_{Abu}$, $D_{(14-38)}$[c] | | $[R]_{Abu}$[d] | |
|---|---|---|---|---|---|
| study | ref | study | ref | study | ref |
| structure, pH 5, 1 °C | *13* | dynamics, pH 4.5, 18 °C | *1* | structure of $[R]_{Abu}$, pH 4.5, 1 °C | *17* |
| thermal unfolding, pH 5 | *12* | dynamics, pH 3.8, 7 °C | *e* | dynamics of $[R]_{Abu}$, pH 5, 1 and 7 °C | *e* |
| dynamics, pH 4.5, 7 °C | *1* | structure of mutants Y23A, Y21A, pH 4.5, 1 °C | *18* | dynamics of $[R]_{Abu}$, pH 3, 7 °C | *e* |
| urea-induced unfolding, pH 5 | *e* | | | | |

[a] Ribbons represent segments where the native structure is retained. Dotted lines indicate unfolded regions, and closed circles indicate the position of the $^{15}N$ labels. [b] PF is an equilibrating ensemble of the partially folded conformations $P_f$ and $P_d$ of $[14-38]_{Abu}$ at pH 4.5−5 and 1−7 °C. [c] D is $[14-38]_{Abu}$ denatured by pH <4 or temperature >15 °C. [d] In $[R]_{Abu}$, BPTI is completely reduced by replacement of all cysteines with Abu. [e] This study.

Fully unfolded $[R]_{Abu}$ shows evidence of nonrandom structure, and is more compact than a 'random coil' (*13*); unfolded variants of $[14-38]_{Abu}$, with single site mutations Y21A or Y23A, also have NMR-detected order (*14*). New data in the present work include NMR-detected dynamics of $[R]_{Abu}$ and of pH-denatured $[14-38]_{Abu}$, referred to as $D_{(14-38)}$. The dynamics of individual residues in an unfolded polypeptide reveal the segments of the chain where mobility is restricted and nonrandom contacts are favored (*1, 15−18*). NMR parameters determined from measurements of $T_1$, $T_2$, and heteronuclear NOEs indicate that in both $D_{(14-38)}$ and $[R]_{Abu}$ some regions of the unfolded chain are more ordered than others. Comparison of $[R]_{Abu}$ to $D_{(14-38)}$ variants shows the effect of the 14−38 disulfide on transient order in the unfolded ensemble.

The second question, regarding the behavior of core residues in partially folded $[14-38]_{Abu}$, must be answered in the context of its conformational heterogeneity. Considerable structural complexity arises from the ensemble nature of the partially folded protein. Since the molecule is synthesized with selective $^{15}N$-labeling at nine positions, each backbone amide $^{15}NH$ is a microscopic probe that samples the array of conformations collectively abbreviated PF (*19*). In the PF ensemble, segmental (local) fluctuations result in interconversion of individual NHs between conformational families $P_f$ and $P_d$ (*1*). $P_f$ and $P_d$ are not different conformations of the molecule. Rather they represent, for a specific amide NH, microscopic families of conformations that are separated by energy barriers sizable enough to give $P_f-P_d$ interconversion rates of less than milliseconds (slow exchange on the NMR time scale). Such barriers may be general for folding intermediates, as conformational exchange broadening is reported for other partially folded proteins (*20−22*). In partially folded $[14-38]_{Abu}$, the most ordered, nativelike structure is in core residues, as detected by NOEs (*23*) and by dynamics (*1*). For individual amide groups in partially folded $[14-38]_{Abu}$, unfolding/folding profiles are non-two-state for temperature (*19*) and urea (reported here) denaturation. In urea-induced unfolding, core residues have a striking difference as compared to noncore residues. In both temperature and urea unfolding of partially folded $[14-38]_{Abu}$, it is significant that a shallow pretransition baseline is observed, implying that $P_f-P_d$ interconversions are not highly temperature or urea dependent.

## MATERIALS AND METHODS

*Sample Preparation.* Synthetic BPTI variants were prepared by automated Fmoc solid-phase synthesis using methods described elsewhere (*24*). The positions of $^{15}N$-labeled backbone amides in various BPTI analogues studied are shown in Table 1 as circles on the polypeptide chains. Not all positions are labeled in every synthesis. Here, $[14-38]_{Abu}$ was prepared as in ref (*1*) with $^{15}N$ at residues 4, 6, 22, 25, 27, 28, 33, 45, and 48. For $[R]_{Abu,}$ $^{15}N$ is incorporated in the peptide amides of the N-terminal helix (Phe 4, Leu 6), in the antiparallel $\beta$-sheet core (Phe 22, Leu 29, Phe 33), in the turn (Ala 25, Ala 27, Gly 28), in the $\beta$-bridge (Phe 45), in the C-terminal helix (Ala 48), and in the flexible loops (Gly 12, Ala 16, Gly 37, Ala 40, Gly 56) (Table 1). Amino acid analyses and electrospray ionization mass spectra of the purified proteins were in good agreement with theoretical values.

$^{15}N$-$D_{(14-38)}$ was prepared at pH 3.5 by dialysis in 50 mM acetate buffer. At this pH, there is no stable secondary structure detected by either CD or NMR. $[R]_{Abu}$ samples were dialyzed in 50 mM acetate, at either pH 5 or pH 3. All NMR samples were in the concentration range of 0.2−0.4 mM.

Samples for urea denaturation were prepared by dialysis of $^{15}N$-$[14-38]_{Abu}$ in 50 mM acetate buffer, pH 5. The protein was titrated with increasing concentrations of urea (from an 8 M stock solution, exchanged in $D_2O$ and lyophilized). Each sample was allowed to equilibrate overnight to a final concentration of 0−2 M urea before data acquisition at 5 °C.

*NMR Spectroscopy.* Spectra were collected on Varian Inova 500 or 600 MHz spectrometers equipped with triple resonance pulsed field gradient probes. All spectra were acquired with a flip-back pulse sequence utilizing gradients for water suppression and enhanced sensitivity (*25*). Spectra were collected as 2048 × 192 complex matrixes with sweep widths of 7000 and 1800 Hz in the $^1H$ and $^{15}N$ dimensions,

respectively. Data were processed and analyzed using Felix 97.0 (MSI, San Diego). Resolution in $\omega_1$ was increased by linear prediction. Cross-peak intensities were quantified by measuring peak heights of cross-peak slices along the $\omega_2$ axis. A square sinebell window function was used with a 75° shift and a window size of 1024 points in the first dimension, and 192 points in the other dimension.

$T_1$, $T_2$, and heteronuclear NOE experiments were acquired at 7 °C on the 500 MHz spectrometer using pulse sequences described in ref (*26*). Values of $T_1$ were determined from 11 spectra with relaxation delays ranging from 0.05 to 1 s, with 64 scans per increment, and 1.7 s for recycle delay. Values of $T_2$ were determined from 9 spectra with relaxation delays ranging from 0.01 to 0.23 s, with 64 scans per increment and 1.9 s for recycle delay. Steady-state $^1$H-$^{15}$N NOEs were determined from pairs of spectra recorded in the presence and absence of amide proton saturation with 128 increments of 192 scans each. Spectra recorded with proton saturation utilized a 3 s period of saturation and an additional 1 s delay, while those recorded in the absence of proton saturation were acquired with a relaxation delay of 4 s. Saturation was achieved by the application of a train of 90° pulses separated by 5 ms delay.

For urea denaturation experiments, a total of 10 $^1$H-$^{15}$N HSQC spectra were acquired on the 600 MHz spectrometer at 5 °C with a relaxation delay of 3 s that is sufficiently longer than $T_1$ values to permit quantitative volume integration. At 5 °C, amide nitrogen $T_1$ values of $P_f$ and $P_d$ conformations are on average 0.33 and 0.45 s, respectively (*1*). A total of 64 scans were collected for each time increment.

*Data Analysis.* For relaxation data analysis, values of relaxation time constants, $T_1$ and $T_2$, were determined by fitting the measured peak height vs time profiles to a single-exponential decay function: $I_t = I_0 \exp(-t/T)$, where $t$ is the variable relaxation delay, $I_t$ is the intensity measured at time $t$, and $I_0$ is the intensity at time zero. Uncertainties in the relaxation times were determined from the standard error in the slope of the linear fit of the natural log of $I_t$ vs time. NOE values reported are the average of ratios of peak intensities in the presence and absence of proton saturation obtained from duplicate experiments. For $[R]_{Abu}$ at 7 °C, standard deviations were determined from intensities of the baseline noise in the spectra by integration of noise for each slice of a cross-peak according to the equation: $[(\delta I_A/I_A \times 100)^2 + (\delta I_B/I_B \times 100)^2]^{1/2}$, where $I$ and $\delta I$ denote the intensity of the peak and its baseline noise, respectively, and subscripts A and B refer to spectra recorded in the presence and absence of proton saturation, respectively.

For urea denaturation experiments, spectra of partially folded $[14-38]_{Abu}$ show two sets of peaks: f-peaks report $P_f$, and u-peaks report primarily $P_d$ at 5 °C and low urea concentration. At increasing urea concentration, the u-peaks represent a mixture of $P_d$ and D, and primarily D after unfolding. Since $P_d$ and D conformations cannot be measured independently, because their peaks have the same chemical shift, data for each residue are presented as the ratio of the sum of u-peaks divided by f-peaks (Figure 5). Intensities obtained from peak heights in $^1$H-$^{15}$N HSQC show essentially the same trend as those obtained from peak volumes.

*Spectral Density Functions.* The spectral density function $J(\omega)$ is a frequency distribution function that describes the $^1$H-$^{15}$N bond motions, which are primarily rotational. $J(\omega)$ characterizes the motions of the bond at five frequencies, $\omega = 0$, $\omega_N$, $\omega_H$, and $\omega_N \pm \omega_H$ as shown in eqs 1−3 [reviewed in ref (*27*)]:

$$1/T_1 = (d^2/4)[J(\omega_H - \omega_N) + 3J(\omega_N) + 6J(\omega_H + \omega_N)] + k_{csa}J(\omega_N) \quad (1)$$

$$1/T_2 = (d^2/8)[4J(0) + J(\omega_H - \omega_N) + 3J(\omega_N) + 6J(\omega_H) + 6J(\omega_H + \omega_N)] + (k_{csa}/6)[4J(0) + 3J(\omega_N)] \quad (2)$$

$$\mathrm{NOE} = 1 + (d^2/4)(\gamma_H/\gamma_N)[6J(\omega_H + \omega_N) - J(\omega_H - \omega_N)]T_1 \quad (3)$$

where $k_{csa} = (2/15)\Delta\sigma^2\omega_N^2$ is the chemical shift anisotropy constant, $\Delta\sigma = -160$ ppm is the difference between parallel and perpendicular components of chemical shift tensors, $d = [\mu_0 h\gamma_N\gamma_H/(8\pi^2)]/\langle r_{NH}^{-3}\rangle$ is a proportionality constant, and $\gamma_H$ and $\gamma_N$ are the gyromagnetic ratios of H and N, respectively.

Farrow et al. have shown that terms in eqs 1−3 containing $\omega_H$ and $\omega_N \pm \omega_H$ can be replaced by terms using the frequencies $(0.870\omega_H)$, $(0.921\omega_H)$, and $(0.955\omega_H)$, to yield eqs 4−6 (*26*, *28*). $J(0.92\omega_H)$ and $J(0.955\omega_H)$ are estimated as $(0.870/0.921)^2J(0.870\omega_H)$ and $(0.870/0.955)^2J(0.870\omega_H)$, respectively, and $J(0.870\omega_H)$ is obtained directly from eq 6. For brevity, we will refer to $J(0.870\omega_H)$ simply as $J(\omega_H)$ in the following discussion.

$$1/T_1 = (d^2/4)[3J(\omega_N) + 7J(0.921\omega_H)] + k_{csa}J(\omega_N) \quad (4)$$

$$1/T_2 = (d^2/8)[4J(0) + 3J(\omega_N) + 13J(0.955\omega_H)] + (k_{csa}/6)[4J(0) + 3J(\omega_N)] \quad (5)$$

$$\mathrm{NOE} = 1 + (d^2/4)(\gamma_H/\gamma_N)[5J(0.870\omega_H)]T_1 \quad (6)$$

For error estimation in the spectral density functions, input data sets were generated randomly from $T_1$, $T_2$, and NOE data using the uncertainties of the raw data as standard deviation and assuming a normal distribution. No correction for $R_{ex}$, the millisecond−microsecond chemical exchange contribution to the transverse relaxation rate, has been incorporated in determination of the values of the spectral density functions.

## RESULTS

*Dynamics of $D_{(14-38)}$.* In $[14-38]_{Abu}$, the single disulfide bond, 14−38, links two loops near the trypsin binding site. $[14-38]_{Abu}$ is partially folded at pH 4.5 and 1−7 °C, and is globally denatured by raising the temperature above 20 °C at pH 5 (*19*), or by lowering the pH to <4 at 7 °C (*10*). $^1$H-$^{15}$N HSQC spectra of pH-denatured $[14-38]_{Abu}$ [hereafter called $D_{(14-38)}$] at 7 °C show peak distributions similar to spectra obtained for thermally denatured $[14-38]_{Abu}$ (*19*). The low chemical shift dispersion and the absence of a CD signal at 220 nm confirm that $D_{(14-38)}$ is a denatured ensemble. Dynamic experiments on $D_{(14-38)}$ were performed at the same temperature as earlier experiments on partially folded $[14-38]_{Abu}$ (*1*).

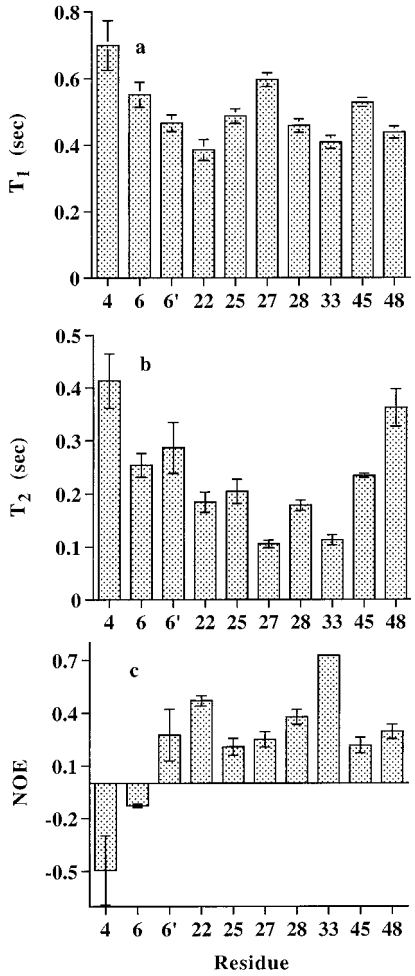


FIGURE 1: Plots of $^{15}N$ $T_1$, $T_2$, and steady-state $^1H$-$^{15}N$ NOEs recorded for $D_{(14-38)}$ at pH 3.5 and 7 °C. For residue 6, two bars are shown for conformations that are both disordered. (See text for further discussion.) Similar data quality was obtained for the other variants.

In native BPTI, the slow exchange core corresponds to the central antiparallel $\beta$-sheet spanning residues 18−35, which contains a number of hydrophobic side chains (2 Ile, 3 Tyr, 2 Phe) and a reverse-turn (25−28), along with a $\beta$-bridge (44−45). In partially folded $[14-38]_{Abu}$, the central antiparallel $\beta$-sheet is most ordered relative to the rest of the molecule. The $\beta$-bridge and the first turn of the C-terminal helix are also ordered but to a smaller extent (*1*, *19*). When we refer to core residues in the following discussion, the core includes the most ordered residues, and those are residues of the central $\beta$-sheet and the turn.

$T_1$, $T_2$, and steady-state heteronuclear NOE values for nine amide $^{15}NHs$ of $D_{(14-38)}$ at 7 °C were determined (Figure 1). The average $T_1$ value for $D_{(14-38)}$ is 0.5 s (0.4−0.7 s range), somewhat higher than 0.45 s for $P_d$, and 0.33 s for $P_f$ (*1*). $T_2$ values for $D_{(14-38)}$ are considerably longer and of wider variation (0.11−0.38 s) than for $P_f$ (0.06−0.12 s) or $P_d$ (0.07−0.21 s), indicating more disorder and conformational heterogeneity. Residues 22, 27, and 33 have the shortest $T_2$ in both $D_{(14-38)}$ and $P_d$. In $P_d$, $T_2$ values of these residues change as a function of field strength, verifying that they are in the intermediate exchange regime (*1*). We expect, similarly, that line broadening observed for residues 22, 27, and 33 in $D_{(14-38)}$ is also due to millisecond−microsecond time scale motions. Steady-state heteronuclear $^1H$-$^{15}N$ NOEs give an indication of the internal mobility of proteins; high positive or negative NOEs imply rigid or flexible amide N−H bond vectors, respectively. The correlation times obtained for $P_f$ and $P_d$ are 8 and 10 ns, respectively (*1*); the estimated correlation time for a folded protein of this size at 7 °C is 8 ns (*27*). On this time scale, NOE values are most sensitive to protein backbone dynamics. In $D_{(14-38)}$, NOEs range from negative values for residues 4 and 6, to high positive values for residues 22 and 33, about 2-fold higher than the NOEs of other residues. When compared to $P_d$ and $P_f$ of the same NH in partially folded $[14-38]_{Abu}$, positive NOEs in $D_{(14-38)}$ at 7 °C (0.35) are, on average, comparable to those in $P_d$ (0.34) and significantly lower than in $P_f$ (0.60).

Spectral density functions, $J(\omega)$, describe rotational fluctuations of the $^1H-^{15}N$ bond vectors. $J(\omega)$ values at three frequencies, $\omega = 0$, $\omega_N$, and $0.870\omega_H$, were evaluated where $\omega_H$ and $\omega_N$ are the Larmor frequencies of the $^1H$ and $^{15}N$ nuclei. Spectral densities at these frequencies reflect the range of time scales of the N−H bond vector motions. Bonds with more rapid reorientation are expected to have a wider distribution of frequencies, with more contribution from high-frequency modes (*29*). As a result, greater order is indicated by higher $J(0)$ and $J(\omega_N)$, and lower $J(\omega_H)$. An increase in the value of $J(0)$ relative to other residues may also be due to motions on the millisecond−microsecond time scale that contribute to transverse relaxation, which were not factored out in our analysis. We consider residues with a noticeably higher value of $J(0)$ relative to other residues, that are not accompanied by higher $J(\omega_N)$, and lower $J(\omega_H)$, to be in intermediate chemical exchange.

Figure 2 shows spectral density functions for several denatured BPTI analogues: $D_{(14-38)}$ at pH 3.5 and 7 °C (a−c), $[R]_{Abu}$ at pH 5 and 1 °C (d−f), $[R]_{Abu}$ at pH 5 and 7 °C (g−i), and $[R]_{Abu}$ at pH 3 and 7 °C (j−l). In $D_{(14-38)}$, $J(0)$ values are the highest for residues 27 and 33, $J(\omega_N)$ values are the highest for residues 22 and 33, and $J(\omega_H)$ is lowest for residue 33. This indicates that residues 22 and 33 are most ordered on the fast time scale and residue 27 is most ordered on the intermediate exchange time scale. The highest order for residues 22 and 33 is also reflected in the high positive heteronuclear NOEs (Figure 1c). Other residues have sizable positive NOEs but not to the same extent (~2-fold less). In $[R]_{Abu}$, the no-disulfide variant at similar solution conditions and at the same temperature (Figure 2g−i), $J(0)$ values for various residues measured are similar and significantly smaller than $J(0)$ of $D_{(14-38)}$. Similarly, higher $J(\omega_N)$ and lower $J(\omega_H)$ are observed for $D_{(14-38)}$ compared to $[R]_{Abu}$.

We use the reduced spectral density mapping approach because it requires few assumptions about the form of the motion of the protein and is suitable for analysis of nonglobular denatured proteins (*28*). Since relaxation is dominated by dipole−dipole interactions between $^{15}N$ and the attached proton spin, motional parameters of $D_{(14-38)}$ and $[R]_{Abu}$ are extracted independently of their structure. Because $T_1/T_2$ ratios vary significantly among residues, a single correlation time cannot describe the overall tumbling of the entire protein. Hence, we did not analyze the data using the model-free spectral density function, where an assumption of a single correlation time is required (*30*).

*Dynamics of the Fully Reduced BPTI Analogue, $[R]_{Abu}$.* $[R]_{Abu}$, with all six cysteines replaced by Abu, has no NMR-

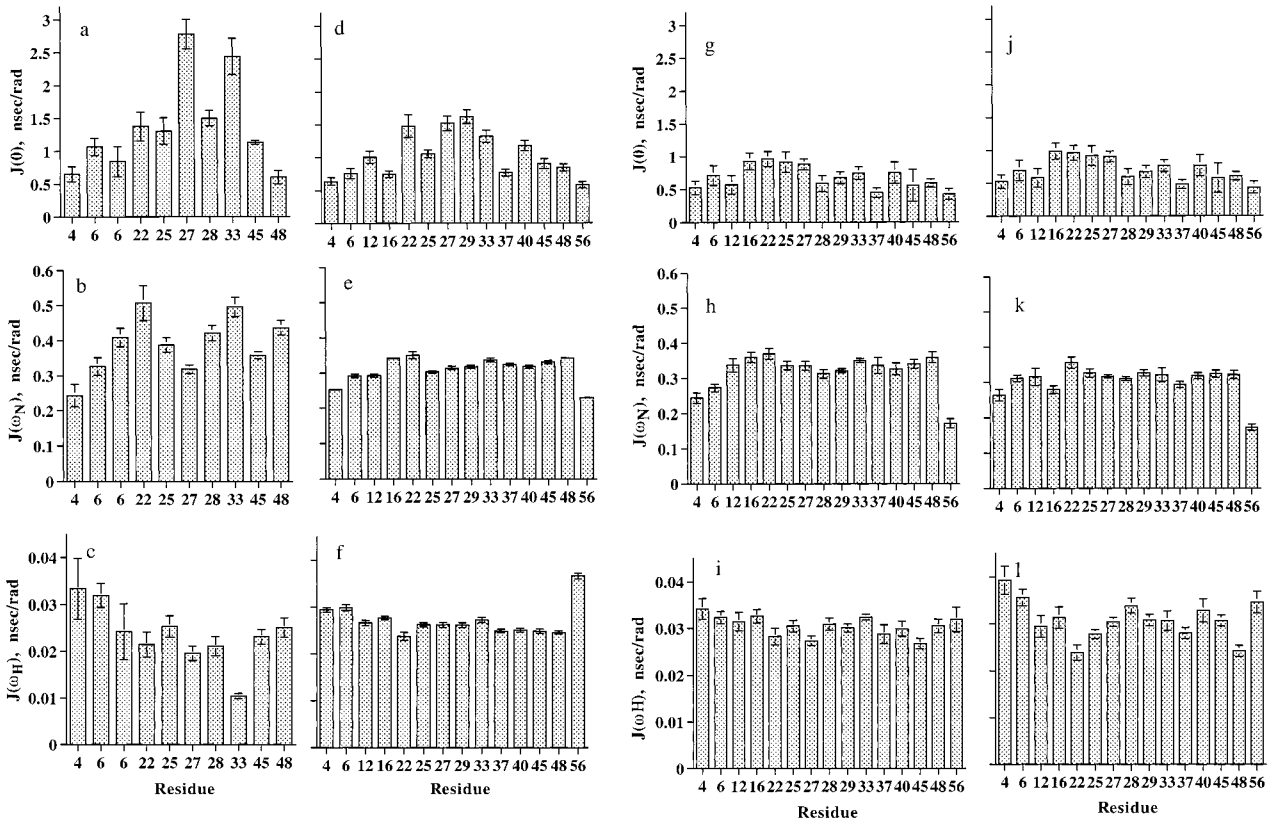


FIGURE 2: Spectral density values in ns/rad for $D_{(14-38)}$ at pH 3.5 and 7 °C (a−c), $[R]_{Abu}$ at pH 5 and 1 °C (d−f), $[R]_{Abu}$ at pH 5 and 7 °C (g−i), and $[R]_{Abu}$ at pH 3 and 7 °C (j−l). Residues in $D_{(14-38)}$ have more heterogeneous dynamics than in $[R]_{Abu}$ at all conditions. For example, in frame a, residues 27 and 33 have noticeably higher $J(0)$ relative to other residues, indicating slower fluctuation due to intermediate exchange.

Table 2: Average Spectral Density Functions (in ps/rad) for Partially Folded and Unfolded BPTI Analogues[a]

| | $P_f$ (pH 5.0, 7 °C) | $P_d$ (pH 5.0, 7 °C) | $D_{(14-38)}$ (pH 3.5, 7 °C) | $[R]_{Abu}$ (pH 5.0, 1 °C) | $[R]_{Abu}$ (pH 5.0, 7 °C) | $[R]_{Abu}$ (pH 3.0, 7 °C) |
|---|---|---|---|---|---|---|
| $\langle J(0)\rangle$[b] | 3179 ± 242 | 2612 ± 224 | 1368 ± 164 | 1026 ± 80 | 684 ± 121 | 695 ± 118 |
| $\langle J(\omega_N)\rangle$ | 632 ± 65 | 437 ± 46 | 390 ± 25 | 310 ± 5 | 318 ± 14 | 304 ± 11 |
| $\langle J(0.87\omega_H)\rangle$ | 19 ± 3 | 28 ± 6 | 24 ± 3 | 27 ± 1 | 31 ± 1 | 31 ± 2 |

[a] Spectral density values are based on data obtained in (*1*). [b] Large values of $J(0)$ and $J(\omega_N)$ indicate more order, while large $J(0.87\omega_H)$ indicates less order.

or CD-detected secondary or tertiary structure; however, it does show NOE evidence of nonrandom structure (*13*), and hydrodynamic evidence of collapse at pH 5 and 1 °C (*31*). In dynamic experiments under the same conditions, residues 22, 27, 29, 33, and 40 in $[R]_{Abu}$ have $J(0)$ values somewhat higher than the rest (Figure 2d), indicating the presence of nonrandom structure sampled by motions on the intermediate−fast time scale. Values of $J(0)$ at 1 °C are significantly higher on average than those at 7 °C and pH 3 (Figure 2g,j, and Table 2). Values of $J(\omega H)$ for $[R]_{Abu}$ at 7 °C and pH 3 (Figure 2i,l) are somewhat higher than those for $[R]_{Abu}$ at pH 5 and 1 °C (Figure 2f). Interestingly, residues 22 and 48 have the smallest values of $J(\omega H)$ for $[R]_{Abu}$ at pH 3 (Figure 2l), indicating that these residues are more ordered relative to the rest. Figure 3 compares heteronuclear NOEs for partially folded $[14-38]_{Abu}$ at 7 °C (a), $D_{(14-38)}$ at 7 °C (b), $[R]_{Abu}$ at 1 °C (c), and $[R]_{Abu}$ at 7 °C (d) at pH 5 (stippled bars) and pH 3 (dark bars). For $[R]_{Abu}$ at 1 °C, small positive NOEs are observed for residues 22, 37, 40, 45, and 48, while terminal residues 4, 6, 12, and 56 have negative or near-zero NOEs. The small positive NOEs indicate nonrandom structure at 1 °C that is highly unstable and is almost completely lost at 7 °C (Figure 3d), with most residues showing strong negative NOEs indicating complete disorder. It is notable that residues 22, 27, 45, and 48 have either slightly positive NOEs or smaller negative NOEs than the rest of the molecule, indicating that even when most of the nonrandom structure is lost, these residues are least flexible. At lower pH, slightly more flexibility is observed, except for residues 22 and 48.

Figure 4 compares the flexibility in the $[R]_{Abu}$ chain measured as the ratio of spectral density functions $J(\omega N)/J(\omega H)$ at two temperatures: 1 °C (closed circles) and 7 °C (open circles). Higher ratios, reflecting higher $J(\omega N)$ or lower $J(\omega H)$, or both, imply more order. At 1 °C, residues 22, 45, and 48 have the highest order. These residues are also the least flexible at 7 °C and pH 3 as shown by the lowest $J(\omega H)$ for residues 22 and 48 (Figure 2l).

*Urea Denaturation of Partially Folded [14−38]$_{Abu}$.* Under conditions where $[14-38]_{Abu}$ is partially folded, each $^{15}N$-labeled amide in $^{1}H$-$^{15}N$ HSQC spectra has peaks corresponding to two or more slowly interconverting conformations. Their interconversion rate constants are slow on the NMR time scale (0.045−0.88 $s^{-1}$), resulting in separate

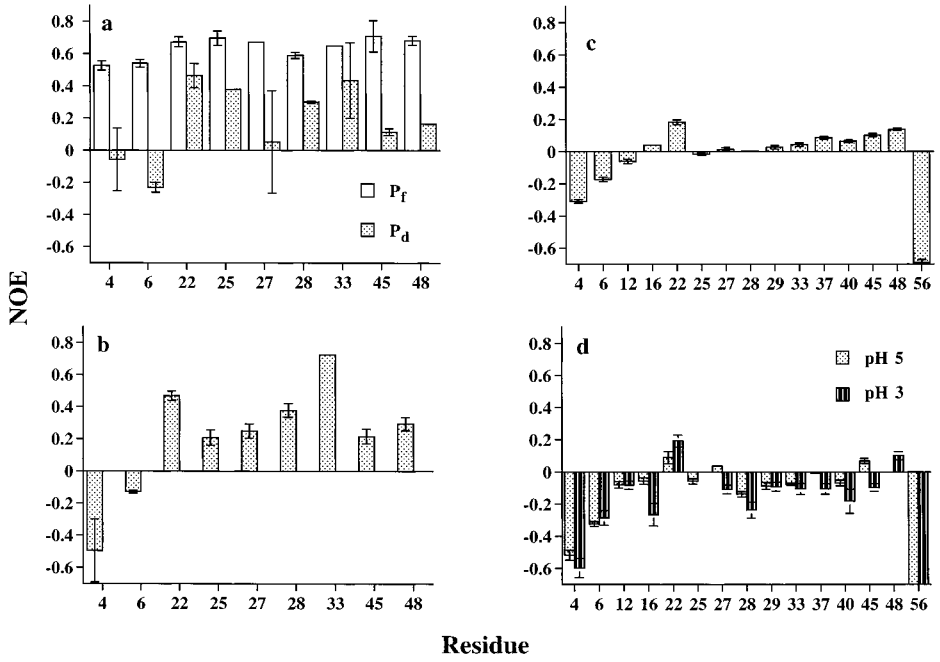


FIGURE 3: Comparison of $^1H$-$^{15}N$ heteronuclear NOEs for partially folded and unfolded BPTI analogues. (a) $[14-38]_{Abu}$, PF, at pH 5 and 7 °C is reproduced from (*1*); (b) $D_{(14-38)}$, at pH 3.5 and 7 °C; (c) reduced BPTI, $[R]_{Abu}$, at pH 5 and 1 °C; (d) $[R]_{Abu}$ at 7 °C and pH 5 (stippled bars), and at 7 °C and pH 3 (solid bars).

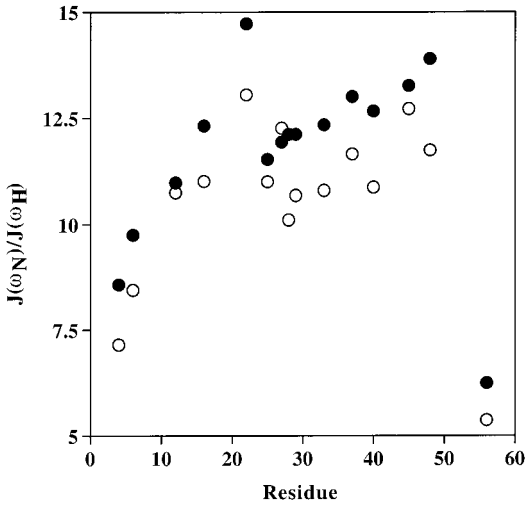


FIGURE 4: Ratios of spectral density functions $J(\omega_N)/J(\omega_H)$ of $[R]_{Abu}$ at pH 5 and 1 °C (closed circles) and 7 °C (open circles). Higher ratios are observed at the lower temperature, reflecting higher $J(\omega_N)$ and lower $J(\omega_H)$ values, and indicating more order, especially for residues 22 and 48.

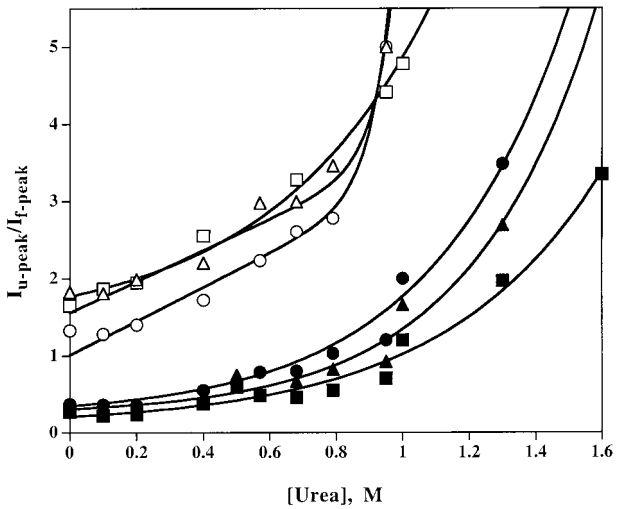


FIGURE 5: Urea unfolding curves for individual residues in partially folded $[14-38]_{Abu}$, shown as the ratio of u-peak to f-peak intensity as a function of urea concentration. The lines are to show a general trend and are not derived from a specific curve-fitting procedure. Data are presented for core residues Phe 22, Phe 33, and Ala 27 (closed circles, squares, and triangles, respectively), for residues Leu 6 and Ala 48 of the N- and C-terminal helices (open circles and triangles, respectively), and for turn residue Ala 25 (open squares).

peaks, f and u, which are assigned to $P_f$ and $P_d$ conformational families by chemical shift and NOE criteria (*1*, *19*). Figure 5 shows urea unfolding profiles at 5 °C for residues 6, 22, 25, 27, 33, and 48 where the ratio of the intensity of the u-peak to the f-peak is given as a function of urea concentration. Residues at 0 M urea have different ratios, indicating that populations of $P_f$ and $P_d$ vary among segments of partially folded $[14-38]_{Abu}$. Higher ratios imply more $P_d$ relative to $P_f$. For example, at 0 M urea, residue 22 (closed circles) with a ratio of 0.37 is predominantly $P_f$, while residue 6 (open circles) with a ratio of 1.2 is about 50% $P_f$, and residue 25 (open squares) with a ratio of 1.6 is predominantly $P_d$. With increasing urea concentration, a denatured conformation, D, is populated and contributes to the intensity of the u-peak, since for a given NH a chemical shift difference between $P_d$ and D is not observed. Measuring ratios, instead of absolute intensities of f-peaks, gives $P_f$ relative to $P_d$ plus D, and eliminates uncertainties due to dilution. For some residues with multiple u-peaks, the intensities of all u-peaks are summed. For example, this is done for residue 6, for which there are two u-peaks due to cis−trans isomerism of neighboring proline residues (*19*).

For each curve in Figure 5, the last point on the right shows the urea concentration at which the f-peak is still measurable. Varying concentrations of urea are required to completely unfold different protein segments, indicating that global denaturation is not two-state. For example, at ~1 M urea,

the f-peak intensities of residues 48 and 6 (open triangles and circles) are miniscule, while the f-peak intensities of other residues are measurable. Two groups of residues are distinguished based on their unfolding profile. Core residues 22 and 33, along with turn residue 27, are 30−50% $P_f$ at ~1.2 M urea (intensity ratio 1−1.6), while residues 6 and 48 in the N- and C-terminal helices and turn residue 25 are completely unfolded.

## DISCUSSION

*Order in Unfolded BPTI Analogues Detected by Relaxation Measurements.* NMR studies on a number of unfolded proteins show that they are highly flexible, exhibit heterogeneous dynamics, and have central residues which are less mobile than those at the termini (*1, 15*−*18, 20*). The level of backbone motion is closely linked to the amount of secondary or residual structure. Dynamic measurements also identify nonrandom regions of a protein as those exhibiting intermediate exchange line broadening; these are suggested to be probable folding nucleation sites (*20*).

Characterization of order in an unfolded protein by NMR dynamic methods involves surveying the time scales of conformational fluctuations. In $D_{(14-38)}$, a pH-denatured form of $[14-38]_{Abu}$, there is considerable order on the intermediate time scale (millisecond−microsecond) as reflected in high $J(0)$ values for Ala 27 and Phe 33 (Figure 2a). Phe 22 and Phe 33 have the highest order on the fast time scale (nanosecond−picosecond) as shown by high positive NOE values (Figure 1c). Both slow and fast dynamic parameters of $D_{(14-38)}$ show that Phe 22, Ala 27, and Phe 33 have the most restricted motion, and hence are likely to be involved in folding initiation, presumably of the antiparallel central $\beta$-sheet. $D_{(14-38)}$ is compared to $P_f$ and $P_d$ conformations of partially folded $[14-38]_{Abu}$ in Figure 3a,b, and Table 2. $D_{(14-38)}$ is considerably less ordered than $P_f$, but shows heteronuclear NOEs similar to $P_d$. $J(0)$ and $J(\omega_N)$ of $P_f$ and $P_d$ observed in partially folded $[14-38]_{Abu}$ are significantly higher than in either $D_{(14-38)}$ or $[R]_{Abu}$. This is not surprising since in partially folded $[14-38]_{Abu}$ the central $\beta$-sheet and the first turn of the C-terminal helix are highly populated ($P_f$ conformations), while $D_{(14-38)}$ and $[R]_{Abu}$ have no detectable secondary structure. Is the order in $D_{(14-38)}$ detected by dynamics nativelike? Although we cannot be certain, it seems possible based on previous work showing that an unfolded species with the 14−38 cross-link has nativelike short- and medium-range NOEs, and no detectable non-nativelike NOEs (*14*).

Although $[R]_{Abu}$, with no disulfide cross-links, is more disordered than $D_{(14-38)}$, its dynamics show intimations of order. In $[R]_{Abu}$, there is restricted mobility at 1 °C, consistent with its previously characterized nonrandom structure at 1 °C and pH 4.5 (*13, 31*). Order is most pronounced in residues 22 and 48, indicated by the highest ratios of spectral density functions relative to the rest of the molecule (Figure 4). To a smaller extent, residues 37, 40, and 45 are also ordered on the fast time scale (positive NOEs in Figure 3c), and residues 27, 29, and 33 are ordered on the intermediate exchange time scale [higher $J(0)$ relative to other residues in Figure 2d]. Mobility is restricted not only for residues of the central $\beta$-sheet core (22, and to a lesser extent 29 and 33), but also for residue 48 which is outside the core. At 7 °C, the order observed at 1 °C is lost (Figure 2g−l and Figure 3d). Even at conditions where $[R]_{Abu}$ appears to be fully disordered by NMR criteria (Figure 3d), residues 22, 25, 27, 45, and 48 show near-zero NOEs, indicating restriction in motion relative to the rest of the molecule.

Is some of the dynamics-detected order in $[R]_{Abu}$ nativelike? An affirmative answer to this question is supported by the report that reduced BPTI still binds and inhibits trypsin, presumably due to a small population of nativelike conformers that are recognized by the protease (*32*). In these experiments, BPTI was fully reduced in DTT, and its binding was conducted at pH 3.5−4.0 at 22 °C, at conditions where we show almost complete disorder (Figure 3d). The presence of trypsin may induce stabilization of nativelike structure, and shift the equilibrium toward a larger population of ordered conformers.

*The 14*−*38 Disulfide Orders the Unfolded Ensemble.* The dynamics of $[R]_{Abu}$ and $D_{(14-38)}$ measured under comparable temperature and buffer conditions allow us to assess the effect of the 14−38 cross-link on ordering unfolded BPTI. Residues in $D_{(14-38)}$ in general show significantly more order than those in $[R]_{Abu}$ at similar conditions (Figure 3b,d). Residues 22, 27, and 33, which are not close to the 14−38 cross-link, are clearly the most ordered (Figures 2a and 3b). While $[R]_{Abu}$ in general is significantly less ordered, residues 22 and 48 are somewhat less flexible relative to the rest of the chain (Figure 3d, dark bars), and several others, 37, 40, and 45, increase in order at lower temperature (Figure 3c). In the absence of the 14−38 cross-link, core residue 22 is still the most ordered; other residues outside the slow exchange core, 27, 40, 45, and 48, also show some restriction in mobility. It appears that the primary effect of the 14−38 cross-link is to favor order in residues in the slow exchange core even before secondary structure is stabilized.

The relative ordering of residues, as illustrated most clearly in steady-state heteronuclear NOEs, is consistent with NOE data obtained from 2D NOESY spectra (*13, 14*). Medium- and short-range NOEs in $[R]_{Abu}$ and unfolded $[14-38]_{Abu}$ mutants show that the residues involved in transient interactions correspond mostly to the slow exchange core in native BPTI. Moreover, in the absence of the disulfide, both native and non-native NOEs were observed, while in the presence of the disulfide in the unfolded $[14-38]_{Abu}$ mutants, non-native NOEs were absent and were replaced by native NOEs. This led us to propose that the 14−38 disulfide eliminates the non-native interactions that are populated in $[R]_{Abu}$, and favors nativelike interactions that are in the core and not in the vicinity of the cross-link. More dynamic-detected order hence likely arises from the removal of most fully extended conformations to give the more compact, 14−38-linked ensemble in which ordered conformations in the core are relatively more populated.

In native BPTI, the 14−38 disulfide has very little effect on the dynamic-detected order in residues that are not directly attached to the cross-link, but considerably slows down fluctuations in a destabilized mutant, Y35G (*33*). The change in dynamics as the 14−38 cross-link is formed in Y35G is not surprising since replacement of Tyr 35 with Gly causes rearrangement in the vicinity of the mutation, especially the loops connected by the 14−38 cross-link (*34*). In unfolded BPTI as we show in this work, the formation of the 14−38 disulfide causes a large change in dynamics in residues that

are distant from the cross-link. The role of the disulfide at early stages in BPTI folding apparently is to restrict conformational space and lower the entropic barrier for formation of the native core, while the same disulfide in an otherwise folded protein has a much smaller effect.

We think it likely that any one of the native S−S cross-links, when present as the only disulfide in unfolded BPTI variants, will similarly favor order in the core. In partially folded BPTI mutants, the structure detected for any one-disulfide variant includes a native-like core (*35*, *36*). This would, in large part, account for why the order of disulfide bond formation is not a critical issue in folding.

*In Partially Folded [14−38]$_{Abu}$, the Most Urea-Stable Residues Are in the Native Slow Exchange Core.* The urea denaturation curves in Figure 5 are microscopic profiles obtained for specific $^{15}$N-labeled amide groups. For each $^{15}$NH in partially folded [14−38]$_{Abu}$, two (and in one case three) separate NMR peaks are observed. Based on analysis of these multiple peaks and other experiments (*1*, *19*), we conclude that the partially folded ensemble, PF, undergoes segmental, or noncooperative local fluctuations between $P_f$ and $P_d$, two families of conformations that are, respectively, more folded and more disordered. $P_f$ and $P_d$ each consists of multiple conformers that interconvert rapidly (fast and intermediate chemical exchange in NMR terms). Conformational interchange is slow between $P_f$ and $P_d$, and fast within $P_f$ and $P_d$. The ratio of $P_f$ to $P_d$ and the degree to which $P_f$ is nativelike, and $P_d$ is random coil-like, vary from NH to NH. For NHs in core residues, $P_f$ conformations are highly nativelike and $P_d$ conformations are not entirely random coil. Outside the core, $P_f$ conformations are not entirely nativelike, and $P_d$ conformations are indistinguishable from random coil. $P_f$ conformations of residues near the 14−38 disulfide are relatively disordered, while $P_f$ conformations are nativelike for core residues which are relatively distant from the disulfide. Microscopic conformational families such as $P_f$ and $P_d$, evident in the presence of slow or intermediate exchange peaks in NMR spectra, may be general for partially folded proteins as intermediate exchange is also reported for other partially folded proteins (*21*).

Like thermal unfolding (*19*), urea denaturation of partially folded [14−38]$_{Abu}$ is clearly not two-state. Of the $^{15}$N-labeled residues, core and turn residues Phe 22, Ala 27, and Phe 33 require the highest urea concentration to unfold (Figure 5). For these residues, a significant population of $P_f$ persists at ∼1 M urea, while Ala 48 and Leu 6 are almost completely unfolded. In native BPTI and in $P_f$ conformations of partially folded [14−38]$_{Abu}$, residues 22 and 33 are in the core antiparallel strands, and residue 27 is ordered in the turn connecting the strands. Phe 22 and Phe 33 face each other across the $\beta$-sheet, and Ala 27 is in a turn with a hydrogen bond between its NH and the carbonyl of Asn 24. In partially folded [14−38]$_{Abu}$, the hydrogen bond between residues 24 and 27 is still intact (as judged by NOEs), giving rise to a higher $P_f$ population of Ala 27 relative to other turn residues (*19*). Ala 25 has an unfolding profile similar to other core residues, but has a Pf population similar to Ala 48 and Leu 6. The variation in urea concentration needed to fully denature different protein segments corroborates the concept of partially folded BPTI as an ensemble of interconverting species undergoing segmental fluctuation (*11*, *37*). The higher stability of residues 22, 27, and 33 implies that in the partially folded [14−38]$_{Abu}$ ensemble, there is preferential stabilization of interactions among residues that fold into the core of native BPTI.

## CONCLUSIONS

The structure and dynamics of synthetic BPTI variants, which are equilibrium models of species populated at the onset and during folding, have been characterized. In unfolded BPTI analogues, $D_{(14-38)}$, and in $[R]_{Abu}$, there is evidence of a developing core even though no secondary structure is detected by NMR or CD. Dynamic parameters measured for selected $^{15}$N-labeled sites indicate variation in the relative order/disorder between proteins and between different residues within the same protein. The highest order in $D_{(14-38)}$ is for residues that are in the central $\beta$-sheet slow exchange core of the native protein. $[R]_{Abu}$ is significantly less ordered in general, but has detectable order in non-contiguous residues such as 22 and 48.

Comparison of $D_{(14-38)}$ and $[R]_{Abu}$ indicates that in the unfolded ensemble the 14−38 disulfide enhances a bias toward more order in residues that fold into the native core. In partially folded [14−38]$_{Abu}$, microscopic families of conformations separated by significant energy barriers are detected for each NH, with the highest degree of order and the most nativelike structure observed in residues which in native BPTI fold into the slow-exchange core (*1*, *23*). Here we show that core residues in partially folded [14−38]$_{Abu}$ are significantly more stable to urea denaturation than other residues.

The NMR-detected structure and dynamics of partially folded and unfolded BPTI analogues, reported here and previously, collectively show that core residues in the most stable part of the folded protein are most nativelike and stable in partially folded conformations, and most ordered in unfolded conformations.

## REFERENCES


1. Barbar, E., Hare, M., Daragan, V., Barany, G., and Woodward, C. (1998) *Biochemistry 37*, 7822−7833.
2. Dill, K. A., and Chan, H. S. (1997) *Nat. Struct. Biol. 4*, 10−19.
3. Dobson, C. M., Sali, A., and Karplus, M. (1998) *Angew. Chem., Int. Ed. Engl. 37*, 868−893.
4. Klimov, D. K., and Thirumalai, D. (1998) *J. Mol. Biol. 282*, 471−492.
5. Shortle, D. R. (1996) *Curr. Opin. Struct. Biol. 6*, 24−30.
6. Dyson, H. J., and Wright, P. E. (1998) *Nat. Struct. Biol. 5*, 499−503.
7. Brockwell, D. J., Smith, D. A., and Radford, S. E. (2000) *Curr. Opin. Struct. Biol. 10*, 16−25.
8. Falzone, C. J., Mayer, M. R., Whiteman, E. L., Moore, C. D., and Lecomte, J. T. (1996) *Biochemistry 35*, 6519−6526.
9. Ruizsanz, J., Gay, G. D., Otzen, D. E., and Fersht, A. R. (1995) *Biochemistry 34*, 1695−1701.
10. Ferrer, M., Barany, G., and Woodward, C. (1995) *Nat. Struct. Biol. 2*, 211−218.
11. Barbar, E. (1999) *Biopolymers 51*, 191−207.
12. Li, R., and Woodward, C. (1999) *Protein Sci. 8*, 1571−1590.
13. Pan, H., Barbar, E., Barany, G., and Woodward, C. (1995) *Biochemistry 34*, 13974−13981.
14. Barbar, E., Barany, G., and Woodward, C. (1996) *Folding Des. 1*, 65−76.
15. Bhattacharya, S., Falzone, C. J., and Lecomte, J. T. J. (1999) *Biochemistry 38*, 2577−2589.
16. Farrow, N. A., Zhang, O. W., Formankay, J. D., and Kay, L. E. (1997) *Biochemistry 36*, 2390−2402.

17. Sinclair, J. F., and Shortle, D. (1999) *Protein Sci. 8*, 991−1000.
18. Fong, S., Bycroft, M., Clarke, J., and Freund, S. M. V. (1998) *J. Mol. Biol. 278*, 417−429.
19. Barbar, E., LiCata, V., Barany, G., and Woodward, C. (1997) *Biophys. Chem. 64*, 45−57.
20. Frank, M. K., Clore, G. M., and Gronenborn, A. M. (1995) *Protein Sci. 4*, 2605−2615.
21. Schulman, B. A., Kim, P. S., Dobson, C. M., and Redfield, C. (1997) *Nat. Struct. Biol. 4*, 630−634.
22. Alexandrescu, A. T., Evans, P. A., Pitkeathly, M., Baum, J., and Dobson, C. M. (1993) *Biochemistry 32*, 1707−1718.
23. Barbar, E., Barany, G., and Woodward, C. (1995) *Biochemistry 34*, 11423−11434.
24. Barany, G., Gross, C. M., Ferrer, M., Barbar, E., Pan, H., and Woodward, C. (1996) Optimized Methods for Chemical Synthesis of Bovine Pancreatic Trypsin Inhibitor (BPTI) Analogues. in *Techniques in Biochemistry VII* (Marshak, D., Ed.) pp 503−513, Academic Press, San Diego, New York, Boston, London, Sydney, Tokyo, and Toronto.
25. Grzesiek, S., and Bax, A. (1993) *J. Am. Chem. Soc. 115*, 12593−12594.
26. Farrow, N. A., Zhang, O. W., Formankay, J. D., and Kay, L. E. (1995) *Biochemistry 34*, 868−878.
27. Daragan, V. A., and Mayo, K. H. (1997) *Prog. Nucl. Magn. Reson. Spectrosc. 31*, 63−105.
28. Farrow, N. A., Zhang, O. W., Szabo, A., Torchia, D. A., and Kay, L. E. (1995) *J. Biomol. NMR 6*, 153−162.
29. Peng, J. W., and Wagner, G. (1994) Investigation of protein motions via relaxation measurements. in *Nuclear Magnetic Resonance, Part C* (James, T. L., and Oppenheimer, N. J., Eds.) pp 563−596, Academic Press, San Diego, CA.
30. Lipari, G., and Szabo, A. (1982) *J. Am. Chem. Soc. 104*, 4546−4559.
31. Pan, H., Barany, G., and Woodward, C. (1997) *Protein Sci. 6*, 1985−1992.
32. Krokoszynska, I., Dadlez, M., and Otlewski, J. (1998) *J. Mol. Biol. 275*, 503−513.
33. Beeser, S. A., Oas, T. G., and Goldenberg, D. P. (1998) *J. Mol. Biol. 284*, 1581−1596.
34. Housset, D., Kim, K. S., Fuchs, J., Woodward, C., and Wlodawer, A. (1991) *J. Mol. Biol. 220*, 757−770.
35. Van, M. C., Darby, N. J., and Creighton, T. E. (1992) *Proc. Natl. Acad. Sci. U.S.A. 89*, 6775−6779.
36. Staley, J. P., and Kim, P. S. (1992) *Proc. Natl. Acad. Sci. U.S.A. 89*, 1519−1523.
37. Woodward, C., Barbar, E., Carulla, N., Battiste, J., and Barany, G. (2001) *J. Mol. Graphics Modell. 19*, 94−101.

BI010483Z